Magnesium Ions Are Required by *Bacillus subtilis* Ribonuclease P RNA for both Binding and Cleaving Precursor tRNA^{Asp}†

Jane A. Beebe,‡ Jeffrey C. Kurz, and Carol A. Fierke*

Department of Biochemistry, Box 3711, Duke University Medical Center, Durham, North Carolina 27710

Received April 11, 1996; Revised Manuscript Received June 17, 1996⊗

ABSTRACT: The multiple roles Mg^{2+} plays in ribozyme-catalyzed reactions in stabilizing RNA structure, enhancing the affinity of bound substrates, and increasing catalysis are delineated for the RNA component of ribonuclease P (RNase P RNA) by a combination of steady-state kinetics, transient kinetics, and equilibrium binding measurements. Divalent metal ions cooperatively increase the affinity of *Bacillus subtilis* RNase P RNA for *B. subtilis* tRNA^{Asp} more than 10^3-fold, consistent with at least two additional magnesium ions binding to the RNase P RNA·tRNA complex. Monovalent cations also decrease K_D^{tRNA} and reduce, but do not eliminate, the dependence on magnesium ions, demonstrating that nonspecific electrostatic shielding is not sufficient to explain the requirement for high salt. Both di- and monovalent cations promote the high affinity of tRNA by forming contacts in the binary complex that reduce the dissociation rate constant for tRNA. Additionally, the hyperbolic dependence of the hydrolytic rate constant on the concentration of magnesium with a $K_{1/2} \approx 36$ mM suggests that a third low-affinity divalent metal ion stabilizes the transition state for pre-tRNA cleavage. Furthermore, many (about 100) magnesium ions bind independently to RNase P RNA with higher affinity than the $K_{1/2}$ of any of the functionally characterized magnesium binding sites. Therefore, the magnesium binding sites that have differential affinity in either the "folded" species or binary complex are a small subset of the total number of associated magnesium ions. In summary, the importance of magnesium bound to RNase P RNA can be separated functionally into three crucial roles: at least three sites stabilize the folded RNA tertiary structure [Pan, T. (1995) *Biochemistry 34*, 902−909], at least two sites enhance the formation of complexes of RNase P RNA with pre-tRNA or tRNA, and at least one site stabilizes the transition state for pre-tRNA cleavage.

The enzyme ribonuclease P (RNase P)[1] catalyzes the 5′ maturation of precursor tRNA (pre-tRNA) by promoting the cleavage of a specific phosphodiester bond near the 5′ end, producing 5′-phosphate and 3′-hydroxyl end groups; however, the mechanism of this reaction is still under investigation [reviews in Altman (1989), Pace and Brown (1995), and Pace and Smith (1990)]. Bacterial RNase P is a ribonucleoprotein complex composed of an RNA subunit (about 400 nucleotides) and a protein subunit (about 120 amino acids). Both subunits are essential for *in vivo* activity (Baer et al., 1989; Lumelsky & Altman, 1988; Schledl & Primakoff, 1973); however, the RNA component (P RNA) of the bacterial enzyme catalyzes the reaction in the absence of the protein at high salt conditions, demonstrating that it is catalytic (Guerrier-Takada et al., 1983, 1984). The secondary structure of P RNA has been derived from phylogenetic analysis (Haas et al., 1994), and two three-dimensional structural models for *Escherichia coli* P RNA have been proposed on the basis of phylogenetic and biochemical data (Westhof & Altman, 1994; Harris et al., 1994).

Metal ions, especially divalent ones such as Mg^{2+}, are effective in stabilizing the three-dimensional structures of many types of RNA, including tRNA (Crothers, 1979; Quigley et al., 1978; Saenger, 1984; Bujalowski et al., 1986), the *Tetrahymena* ribozyme (Celander & Cech, 1991; Wang & Cech, 1994; Zarrinkar & Williamson, 1994), and *Bacillus subtilis* P RNA (Pan, 1995). Furthermore, the folding pathway for the formation of the *Tetrahymena* ribozyme includes both Mg^{2+} dependent and Mg^{2+} independent steps (Wang & Cech, 1994; Zarrinkar & Williamson, 1994). In *B. subtilis* P RNA, the formation of folded structure, as assayed by protection from Fe(II)−EDTA cleavage, is cooperatively dependent on the concentration of magnesium with $[Mg^{2+}]_{1/2} = 2-3$ mM (Pan, 1995).

Investigation of the catalytic mechanism of P RNA by measuring steady-state hydrolysis of pre-tRNA has been impeded since the rate-limiting step is tRNA dissociation, not chemical cleavage (Beebe & Fierke, 1994; Reich et al., 1988; Tallsjö & Kirsebom, 1993). This problem has been addressed by single-turnover experiments in which the rate constant of the chemical step is reduced by either substitution of a deoxynucleotide at the cleavage site, replacement of Mg^{2+} with Ca^{2+}, or lowering the reaction pH (Smith & Pace, 1993). Additionally, covalent linkage of P RNA to a pre-tRNA substrate facilitates observation of a single cleavage

† Supported by National Institutes of Health Grant GM 40602. C.A.F. received a David and Lucile Packard Foundation Fellowship in Science and Engineering and an American Heart Association Established Investigator Award. J.A.B. and J.C.K. were supported in part by NIH Training Grants GM 07184 and GM 08487, respectively.

* Author to whom correspondence should be addressed. Phone: (919)-684-2557. Fax: (919)-684-8885.

‡ Present address: Institute for Enzyme Research, University of Wisconsin−Madison, 1710 University Avenue, Madison, WI 53705-4098.

⊗ Abstract published in *Advance ACS Abstracts,* August 1, 1996.

[1] Abbreviations: RNase P, ribonuclease P; Tris, tris(hydroxymethyl)-aminomethane; EDTA, (ethylenedinitrilo)tetraacetic acid; TE buffer, 10 mM Tris (pH 8) and 1 mM EDTA; GTP, guanosine triphosphate; NP40, nonidet P40 or α-(ethylphenyl)poly(ethylene glycol); SDS, sodium dodecyl sulfate; buffer 1, 100 mM $MgCl_2$, 800 mM NH_4Cl, 50 mM Tris-HCl (pH 8.0), 0.05% NP40, and 0.1% SDS, with any variations in [$MgCl_2$] or [NH_4Cl] noted; pre-tRNA, precursor tRNA; 5′P, 5′ precursor tRNA fragment; E or RNase P RNA or P RNA, RNA component of RNase P; cpm, counts per minute.

S0006-2960(96)00870-7 CCC: $12.00

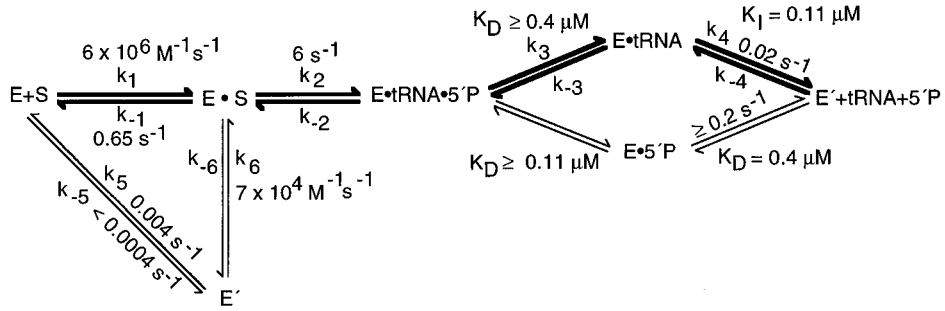

FIGURE 1: Kinetic mechanism for cleavage of pre-tRNA^{Asp} catalyzed by the RNA component of *B. subtilis* RNase P at 37 °C in 100 mM $MgCl_2$, 800 mM NH_4Cl, 50 mM Tris-HCl (pH 8.0), 0.05% NP40, and 0.1% SDS: E, RNA component of RNase P; E′, additional conformer of the RNA component of RNase P; S, pre-tRNA^{Asp}; 5′P, 5′ precursor fragment; and tRNA, mature tRNA^{Asp} (Beebe & Fierke, 1994).

reaction by converting catalysis into an intramolecular reaction (Frank et al., 1994). These experiments demonstrate that the rate constant for pre-tRNA hydrolysis catalyzed by P RNA under single-turnover conditions is dependent on both pH and divalent metal ion concentration (Mg^{2+}, Mn^{2+}, or Ca^{2+}), consistent with hydroxide or metal-bound hydroxide functioning as the nucleophile in the reaction (Smith & Pace, 1993).

An alternative approach for studying the RNase P RNA-catalyzed reaction is the use of transient kinetics to directly measure the hydrolytic rate constant as well as rate and equilibrium constants for association and dissociation of substrate and products. Transient kinetics have been essential in the elucidation of the catalytic mechanisms of other enzymes, including dihydrofolate reductase, fatty acid synthase, mechanochemical ATPases, tryptophan synthase, and DNA polymerase [reviews in Johnson (1986, 1992) and Fierke and Hammes (1995)]. As a requirement for further mechanistic studies of RNase P, a complete kinetic sequence for the cleavage of pre-tRNA^{Asp} catalyzed by the RNA component of RNase P at high concentrations of $MgCl_2$ and NH_4Cl has been elucidated by measuring pre-steady-state, single-turnover, steady-state, and binding kinetics (Figure 1) (Beebe & Fierke, 1994). A minimal kinetic description includes (1) rapid, essentially irreversible binding of pre-tRNA; (2) essentially irreversible cleavage of pre-tRNA; (3) rapid dissociation of the 5′ RNA fragment (5′P); (4) slow dissociation of tRNA; and (5) slow equilibration between two enzyme forms.

Here we assay the functional roles of mono- and divalent cations in the cleavage of *B. subtilis* pre-tRNA^{Asp} catalyzed by *B. subtilis* RNase P RNA by determining the effect of these cations on individual rate constants in the kinetic sequence (Beebe & Fierke, 1994). These data demonstrate that at least two Mg^{2+} binding sites play a key role in stabilizing complexes between *B. subtilis* P RNA and either *B. subtilis* tRNA^{Asp} or pre-tRNA^{Asp} by significantly decreasing the dissociation rate constants. Monovalent cations lessen but do not abolish this dependence. Additionally, a third low-affinity magnesium binding site stabilizes the transition state for pre-tRNA cleavage. However, these functionally determined sites account for only a small fraction of the large number (≈100) of independent Mg^{2+} binding sites in P RNA, which complicates identification of the position of the catalytic metal(s). These experiments delineate the multiple roles of magnesium in the mechanism of the RNase P-catalyzed cleavage and facilitate comparisons to the mechanisms of other ribozymes and nucleases.

MATERIALS AND METHODS

RNA Preparation and Quantitation. The RNA component of RNase P from *B. subtilis* and a precursor of *B. subtilis* tRNA^{Asp} with a mature 3′ end were prepared by *in vitro* transcription reactions as described (Beebe & Fierke, 1994; Milligan & Uhlenbeck, 1989; Reich et al., 1988). T7 RNA polymerase was purified from an overexpressing strain provided by W. Studier (Davanloo et al., 1984). Pre-tRNA was labeled by the addition of [α-^{32}P]GTP to the transcription reaction. To produce mature tRNA^{Asp}, pre-tRNA^{Asp} was cleaved with P RNA and the RNA was then purified by denaturing polyacrylamide gel electrophoresis and quantified by measuring the absorbance at 260 nm (Beebe & Fierke, 1994; Sambrook et al., 1989).

Measurement of Equilibrium and Kinetic Constants for Binding of tRNA and RNase P RNA. Each RNA was resuspended in 10 mM Tris-HCl (pH 8.0) and 1 mM EDTA (TE) (EDTA was not included in experiments containing ≤5 mM $MgCl_2$ in the buffer), heated to 95 °C for 3 min, mixed with an equal volume of 2X buffer 1 (final concentrations of 0−100 mM $MgCl_2$, 0−1.1 M NH_4Cl, 50 mM Tris-HCl (pH 8.0), 0.05% NP40, and 0.1% SDS), and preincubated for 15 min at 37 °C. To measure dissociation constants, P RNA (0−1000 nM) and ^{32}P-labeled mature tRNA^{Asp} (0.1 nM) were incubated together for 1 h at 37 °C. Gel filtration centrifuge columns were prepared and run as described (Beebe & Fierke, 1994; Penefsky, 1979; Sambrook et al., 1989). The gel matrix was separated from the eluate, and the ^{32}P-labeled tRNA contained in each was quantified by scintillation counting. To verify that binding of P RNA and [^{32}P]tRNA^{Asp} reached equilibrium within the allotted time, at 10 and 100 mM $MgCl_2$, the preincubation time was varied from 5 to 60 min, and the incubation time was varied from 30 to 120 min. No change in the fraction of bound tRNA was detected within experimental error, indicating that equilibrium had been reached.

To measure k_{off}, ^{32}P-labeled tRNA^{Asp} (0.1 nM) and P RNA (30−200 nM) were incubated together for 1 h at 37 °C in varied concentrations of $MgCl_2$ (40−100 mM) and NH_4Cl (80−800 mM) such that the concentration of RNase P RNA was more than 10-fold higher than the K_D^{tRNA}. The measurement of the rate constant for tRNA dissociation was initiated by dilution into excess unlabeled tRNA^{Asp} (0.1−1 μM). The RNA was then loaded onto gel filtration centrifuge columns at specific time intervals after dilution, and the counts in the eluate (reflecting tRNA bound to RNase P RNA) were quantified by scintillation counting (Beebe & Fierke, 1994).

Gel shift assays were also performed to measure binding between P RNA and $tRNA^{Asp}$ at low concentrations of magnesium (0−1 mM). The RNA component of RNase P (0−20 μM) and ^{32}P-labeled mature $tRNA^{Asp}$ (0.1 nM) were prepared separately in buffer containing the desired concentration of $MgCl_2$, 50 mM Tris acetate (pH 8.0), 1.1 M NH_4Cl, 0.05% NP40, and 0.1% SDS, as described previously. The P RNA and $tRNA^{Asp}$ were then incubated together for 1 h at 37 °C. A 10X loading buffer containing 40% glycerol and 0.5% xylene cyanol was added, and the samples were loaded onto a 10% polyacrylamide gel while the gel was running at a constant 50 V. Electrophoresis was carried out for about 6 h until the xylene cyanol band migrated ≈0.75 in. (Beebe & Fierke, 1994; Hardt et al., 1993; Pyle et al., 1990) with the gel temperature maintained by circulating 37 °C water through the electrophoresis cell. The ionic strength and magnesium concentration of the gel and running buffer were identical to those of the equilibration buffer [50 mM Tris acetate (pH 8.0), 1.1 M NH_4Cl, and either 0.1 mM EDTA (for no $MgCl_2$) or 1 mM $MgCl_2$] to maintain the equilibrium in the gel well prior to electrophoresis into the gel matrix.

Steady-State Experiments. Experiments were performed under conditions of excess substrate ([S]/[E] ≥ 5). For measurement of steady-state turnover at 5 and 10 mM $MgCl_2$, pre-$tRNA^{Asp}$ and P RNA were dialyzed separately against the reaction buffer for ≈4 h at 37 °C to equilibrate the RNA and magnesium. Reactions were initiated by the addition of P RNA, the mixtures incubated at 37 °C, and the reactions quenched by the addition of an equal volume of 10 M urea, 200 mM EDTA (pH 8.0), 0.1% bromophenol blue, and 0.1% xylene cyanol. Reaction products were separated on an 8% polyacrylamide gel containing 8 M urea and visualized and quantified using a PhosphorImager from Molecular Dynamics (Beebe & Fierke, 1994).

Single-Turnover Experiments. For experiments in which short incubation times (0.005−10 s) were required, a model RQF-3 quench-flow apparatus from Kin-Tek instruments was used as described (Beebe & Fierke, 1994; Johnson, 1986, 1992). The reactions were terminated by mixing with 2.1 volumes of 90 mM EDTA followed by the addition of urea and dyes (bromophenol blue and xylene cyanol) to final concentrations of 4 M and 0.05%, respectively. The reaction products were separated and quantified as described for the steady-state experiments.

Fluorescence Detection Assay for Magnesium. To measure dissociation constants for Mg^{2+} and P RNA, the RNase P RNA was resuspended in TE buffer ([$MgCl_2$] ≥ 2.5 mM) or 10 mM Tris-HCl (pH 8.0) prepared with metal-free deionized water ([$MgCl_2$] < 2.5 mM), heated at 95 °C for 3 min, diluted with an equal volume of 2X buffer, and incubated at 37 °C. RNA was not degraded using these methods, as determined by denaturing polyacrylamide gel electrophoresis followed by staining with ethidium bromide (Sambrook et al., 1989). Sephadex G-50 gel filtration centrifuge columns were prepared in 10 mM Tris-HCl (pH 8.0) and used to separate free magnesium from that bound to RNase P. The concentration of magnesium in the eluate was quantified from fluorescence (excitation = 393 nm, emission = 510 nm; AminoBowman Series 2 luminescence spectrometer) upon the addition of 2 mM 8-hydroxyquinoline-5-sulfonic acid in 4 M guanidine hydrochloride and 0.1 M Tris-SO_4 (pH 9.0) at 25 °C, due to the formation of magnesium−8-quinolinol (Watanabe et al., 1963). The magnesium concentration was determined from a standard curve generated using known concentrations of $MgCl_2$ (linear from 0 to 20 μM).

For experiments involving equilibrium dialysis, the apparatus was sterilized by soaking in 70% ethanol for 30 min, then rinsed with 100% ethanol, and allowed to air dry. Autoclaved dialysis tubing (Scienceware) permeable to molecules with a molecular weight of less than 10 000 was used. The time required to reach equilibrium at 37 °C (7 h) was measured by filling one chamber with buffer 1 lacking magnesium and the other with buffer 1 containing 0.36 mM $MgCl_2$. For all equilibrium dialysis experiments, dialysis proceeded for 7 h at 37 °C. After dialysis, electrophoresis of the RNA indicated that it was not degraded. The dissociation constant for P RNA and Mg^{2+} was calculated from eq 1, where $[L_f]$ is the concentration of Mg^{2+} in the chamber that does not contain P RNA (the concentration of free Mg^{2+}), [E·L] is the concentration of Mg^{2+} bound to P RNA determined from $([L_i] - [L_f])/n$ where $[L_i]$ is the concentration of Mg^{2+} in the chamber containing P RNA and n is the number of moles of Mg^{2+} bound per mole of P RNA, and $[E_f]$ (=$[E_{total}] - [E\cdot L]$) is the concentration of free P RNA (Bell & Bell, 1988).

$$K_D = [L_f][E_f]/[E\cdot L] \quad (1)$$

Data Analysis. Data were fit with the KaleidaGraph (Synergy Software) curve-fitting program using equations described below (Beebe & Fierke, 1994; Cantor & Schimmel, 1980; Fierke & Hammes, 1994; Johnson, 1992). The reported errors are the asymptotic standard errors. Dissociation constants for P RNA and $tRNA^{Asp}$ were determined by fitting the data to eq 2. For measurements of k_{off} for tRNA, the disappearance of radioactivity (cpm) in the eluate was observed and these data were analyzed using eq 3. Steady-state kinetic parameters at high concentrations of magnesium were determined from eq 4, which is complicated by the presence of a slower-binding species of P RNA (Beebe & Fierke, 1994).

$$[tRNA]_{bound}/[tRNA]_{total} = 1/(1 + K_D^{tRNA}/[E]_{total}) \quad (2)$$

$$(cpm)_{eluate} = (cpm)_{total}(e^{-k_{off}t}) \quad (3)$$

$$rate = (A[S] + B[S]^2)/(C + D[S] + E[S]^2) \quad (4)$$

where (see Figure 1)

$$A = k_2k_3k_4(k_1k_5 + k_{-5}k_6)$$

$$B = k_1k_2k_3k_4k_6$$

$$C = k_2k_3k_4(k_5 + k_{-5})$$

$$D = k_4[k_3(k_1k_5 + k_1k_2 + k_{-5}k_6 + k_{-1}k_6) + k_1k_2k_5 + k_2k_{-5}k_6] + k_2k_3(k_1k_5 + k_{-5}k_6)$$

$$E = k_1k_6(k_2k_4 + k_2k_3 + k_3k_4)$$

For single-turnover experiments, the time course for the appearance of products was fit to either a mechanism of a single first-order reaction (eq 5) or two consecutive first-order reactions (eq 6), where t = time and [P] = fraction of

pre-tRNA cleaved = product/(substrate + product) as detected using a PhosphorImager from Molecular Dynamics.

$$[P] = [P]_\infty(1 - e^{-k_{obs}t}) \quad (5)$$

$$[P] = [\text{pre-tRNA}]_o\left[1 + \frac{1}{k_1 - k_2}(k_2 e^{-k_1 t} - k_1 e^{-k_2 t})\right] \quad (6)$$

The number of magnesium binding sites (n) and dissociation constant (K_D) for RNase P RNA and magnesium were determined by fitting the data to eq 7, where ν = moles of Mg^{2+} bound to P RNA per total moles of P RNA. Data were also fit to eq 8, the linearized form of eq 7, commonly known as the equation for a Scatchard plot. Additionally, data were fit using the Hill equation (eq 9), where $f = \nu/n$, $K_{D(min)}/K_D$, $k_{off(min)}/k_{off}$, or $k_{cat}/K_M/(k_{cat}/K_M)_{max}$; α_H is the Hill constant; L is the ligand; and b is the Y-intercept. The accuracy of the value of n obtained from eqs 7 and 8 was checked using eq 10, where the linearity of the plot is very sensitive to the value of n and the slope is $-1/\alpha_H$.

$$\nu = (n[Mg^{2+}]/K_D)/(1 + [Mg^{2+}]/K_D) \quad (7)$$

$$\nu/[Mg^{2+}] = n/K_D - \nu/K_D \quad (8)$$

$$\log[f/(1 - f)] = \alpha_H \log[L] + b \quad (9)$$

$$\ln[Mg^{2+}] = (-1/\alpha_H) \ln[(n/\nu)-1] + \ln K_D \quad (10)$$

RESULTS

Affinity of RNase P RNA for tRNA^{Asp}. We have previously measured the equilibrium and kinetic constants for the binding of $tRNA^{Asp}$ to P RNA at 100 mM $MgCl_2$ and 800 mM NH_4Cl (Beebe & Fierke, 1994). To investigate the importance of monovalent cations in promoting binding between $tRNA^{Asp}$ and P RNA, K_D^{tRNA} was measured as a function of the concentration of NH_4Cl (0−800 mM) at a constant $MgCl_2$ concentration (Figure 2A) using a gel filtration centrifuge column to separate bound and free $tRNA^{Asp}$ (Beebe & Fierke, 1994; Penefsky, 1979; Sambrook et al., 1989). The dissociation constant decreases with increasing ammonium chloride concentration, from 310 nM in the absence of added ammonium chloride to 3 nM at 800 mM NH_4Cl with the midpoint occurring at 6 mM NH_4Cl (Figure 2B). Additionally, a Hill plot of these data (Figure 2B inset, eq 9) has a slope of 1.0 ± 0.1, demonstrating that one NH_4^+ ion (or class of ions[2]) enhances the binding of tRNA to P RNA, consistent with Scheme 1. In this scheme, K_1 and K_3 are determined from the K_D^{tRNA} measured in the presence of zero and saturating NH_4Cl (≥800 mM), respectively. Assuming a single class of sites, the dependence of the observed dissociation constant, $K_{D_{obs}}$, on NH_4Cl concentration can be described by eq 11, yielding the equilibrium constant for dissociation of ammonium from the P RNA·tRNA complex, $K_4 = 6 \pm 1$ mM (Figure 2B). Furthermore, $K_2 = K_1K_4/K_3 \approx 900$ mM to fulfill the equilibrium box shown in Scheme 1.

$$K_{D_{obs}} = K_1(1 + [NH_4^+]/K_2)/(1 + [NH_4^+]/K_4) \quad (11)$$

This enhancement in binding is dependent on the nature of both the cation and the anion, indicating that it is not simply due to an effect on ionic strength. Formation of a complex between P RNA (366 nM) and [^{32}P]$tRNA^{Asp}$ (0.1 nM) was assayed at 37 °C using gel filtration centrifuge columns in the presence of buffer 1 containing 100 mM $MgCl_2$ and either 10 mM NH_4Cl, 10 mM NaCl, or 5 mM $(NH_4)_2SO_4$. Although the ionic strength is constant (0.31−0.33), the fraction of tRNA observed in a bound complex decreases from 0.92 (NH_4Cl) to 0.2 (NaCl) and finally to <0.05 [$(NH_4)_2SO_4$] as the composition of the salt varies. Therefore, substitution of sodium for ammonium or sulfate

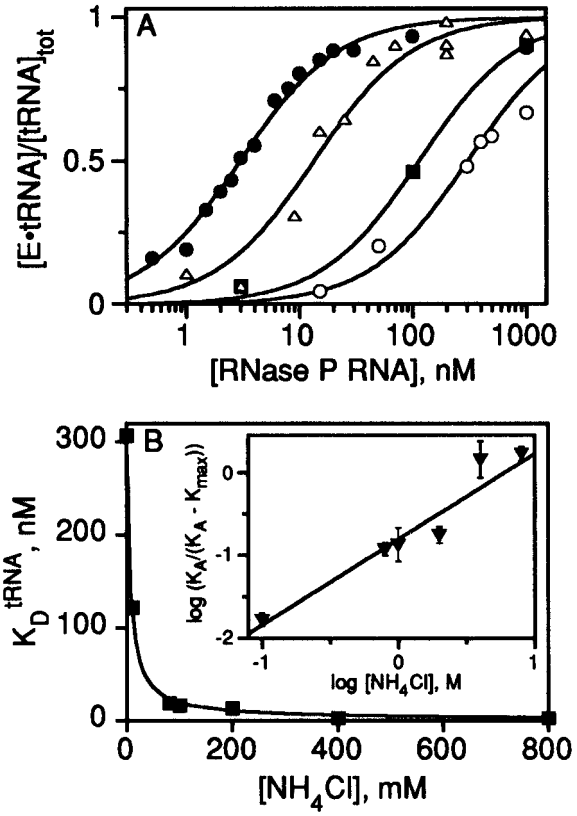

FIGURE 2: Affinity of RNase P RNA for $tRNA^{Asp}$ as a function of NH_4Cl concentration at 100 mM $MgCl_2$. (A) P RNA (0.3−1000 nM) was incubated with ^{32}P-labeled $tRNA^{Asp}$ (0.1 nM) in buffer 1 containing 100 mM $MgCl_2$ and NH_4Cl (0−800 mM) at 37 °C. The fraction of [^{32}P]$tRNA^{Asp}$ bound to P RNA was assayed by radioactivity in the eluate of a Sephadex G-75 centrifuge column. Data were fit to eq 2, yielding the following dissociation constants: 3.0 ± 0.4 nM in 800 mM NH_4Cl (●), 13.5 ± 2.6 nM in 200 mM NH_4Cl (△), 122 ± 21 nM in 10 mM NH_4Cl (■), and 310 ± 130 nM in the absence of NH_4Cl (○). (B) The observed K_D^{tRNA} (■) plotted as a function of the concentration of NH_4Cl. Data were fit with eq 11 from Scheme 1 with $K_1 = 310$ nM and $K_3 = 2$ nM. (inset) Hill plot for the binding of $tRNA^{Asp}$ to P RNA as a function of NH_4Cl concentration (eq 9). A slope of 1.0 ± 0.1 was obtained, demonstrating that one ammonium ion or class of ions promotes binding between P RNA and tRNA.

Scheme 1

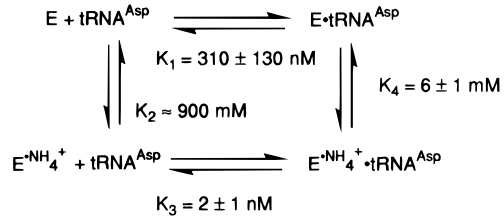

[2] The slope of a Hill plot describes the number of interacting sites but does not distinguish the number of identical, independent sites (Cantor & Schimmel, 1980).

for chloride increases the K_D^{tRNA} approximately 46-fold and >2000-fold, respectively, indicating that the affinity of P RNA for tRNA is dependent on the identity of both the cation and the anion. Similarly, Smith and colleagues (1992) have demonstrated that NaCl and other smaller cations are less effective than NH_4Cl in promoting cross-linking between *E. coli* RNase P RNA and *E. coli* $tRNA^{Phe}$. These results indicate that the effect of ammonium ions on tRNA affinity is not due simply to changes in the effective concentration of the RNAs as a result of the change in ionic strength (Day & Underwood, 1986). Therefore, the enhancement in affinity of P RNA for tRNA caused by NH_4Cl is likely due to an effect on RNA conformation and/or electrostatic interactions. In fact, the data can be interpreted as a single ammonium ion (or independent class of ions) that binds 150-fold more tightly to the E·$tRNA^{Asp}$ complex than to either P RNA or $tRNA^{Asp}$ alone (Scheme 1), perhaps stabilizing a tertiary structure of P RNA with high affinity for tRNA. An ammonium ion binding site that stabilizes tertiary structure has previously been identified in a conserved domain in the *E. coli* large subunit ribosomal RNA (Wang et al., 1993). The ammonium dependence of both rRNA unfolding and the affinity of other ligands, such as ribosomal protein L11, is hyperbolic, although the ammonium dissociation constant is significantly lower for rRNA than P RNA (50 versus 900 mM) (Scheme 1; Draper et al., 1995; Xing & Draper, 1995). Ammonium binding sites may generally stabilize specific tertiary contacts required for the formation of compact RNA structures.

Additionally, the increased K_D^{tRNA} in $(NH_4)_2SO_4$ is consistent with observed decreases in P RNA-catalyzed cleavage of pre-tRNA caused by the substitution of sulfate for chloride (Gardiner et al., 1985; Guerrier-Takada et al., 1986; Pace & Smith, 1990). These data may suggest either that sulfate stabilizes an alternate conformation of P RNA or tRNA (Gardiner et al., 1985; Robinson & Grant, 1966) or that SO_4^{2-} binds competitively to the phosphoryl binding site of P RNA.

Magnesium Is Essential for Binding tRNA. Equilibrium constants for the binding of $tRNA^{Asp}$ and P RNA were measured using gel filtration centrifuge columns at varying concentrations of $MgCl_2$ and a constant ionic strength (0.8−1.1 M NH_4Cl) (Figure 3A). The affinity of P RNA for $tRNA^{Asp}$ is highly dependent on the $MgCl_2$ concentration; dissociation constants range from 3.0 ± 0.4 nM at 100 mM $MgCl_2$ to >1000 nM at 1 mM $MgCl_2$. At low magnesium concentrations, very little bound complex was observed using gel filtration centrifuge columns. To verify this decreased affinity, a gel shift assay was performed (Figure 3B) with the ionic strength and magnesium concentration of the gel and running buffers identical to those of the equilibration buffer; a K_D of 3400 ± 500 nM was determined for the dissociation of $tRNA^{Asp}$ from the P RNA·tRNA complex at 1 mM $MgCl_2$ (Figure 3). Additionally, in the absence of magnesium, <10% bound complex was observed using the gel shift assay at concentrations of P RNA up to 20 μM, suggesting that the $K_D^{tRNA} \geq 180$ μM. Thus, magnesium is essential for binding tRNA tightly to P RNA (Figure 4A); the K_D^{tRNA} decreases at least 10^3-fold and, perhaps, more than 10^5-fold in the presence of saturating Mg^{2+}. Nonspecific electrostatic shielding is not sufficient to explain the requirement for magnesium since the ionic strength is maintained. This observed dependence of tRNA affinity on the concentration of magnesium is comparable to that observed previously using a gel shift assay (Hardt et al., 1993) and much stronger than that measured using a cross-linking assay (Smith et al., 1992). Other divalent cations, such as calcium or manganese, may be substituted for magnesium (Hardt et al., 1993).

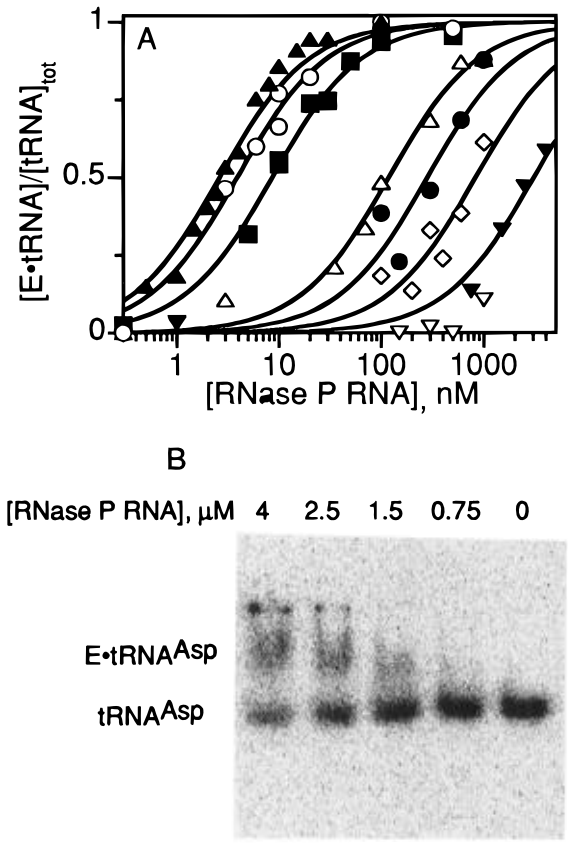

FIGURE 3: Measurement of dissociation constants for [^{32}P]$tRNA^{Asp}$ and RNase P RNA as a function of $MgCl_2$ concentration. (A) P RNA (0.1−1000 nM) was incubated with [^{32}P]$tRNA^{Asp}$ (0.1 nM) at 37 °C in buffer 1 containing 1−100 mM $MgCl_2$ with the ionic strength maintained by varying the NH_4Cl concentration (0.8−1.1 M). The fraction of tRNA bound to P RNA was assayed by monitoring the radioactivity in the eluate of a Sephadex G-75 centrifuge column. Data were fit to eq 2, yielding the following dissociation constants: 100 mM $MgCl_2$ (▲), 3.0 ± 0.4 nM; 70 mM $MgCl_2$ (○), 3.8 ± 0.6 nM; 40 mM $MgCl_2$ (■), 8.6 ± 0.9 nM; 10 mM $MgCl_2$ (△), 119 ± 22 nM; 6 mM $MgCl_2$ (●), 280 ± 50 nM; 3 mM $MgCl_2$ (◇), 833 ± 207 nM; 1 mM $MgCl_2$ (▽), >1000 nM; and 1 mM $MgCl_2$ (▼), 3400 ± 500 nM, as assayed by gel shift described in part B. (B) P RNA (0−4 μM) was incubated with [^{32}P]$tRNA^{Asp}$ (0.1 nM) at 37 °C in buffer 1 containing 1 mM $MgCl_2$/1.1 M NH_4Cl. Free $tRNA^{Asp}$ was separated from E·$tRNA^{Asp}$ on a 10% polyacrylamide gel (see Materials and Methods), and the fraction of bound complex was quantified using a PhosphorImager.

A Hill plot of the dependence of K_D^{tRNA} on the concentration of magnesium (Figure 4B) has a slope of 1.9, suggesting that two Mg^{2+} or classes of Mg^{2+} ions[2] promote binding of *B. subtilis* $tRNA^{Asp}$ to *B. subtilis* RNase P RNA with the midpoint of the transition [$f/(1 - f) = 1$] occurring at 75 mM Mg^{2+}. The simplest model consistent with these data (Scheme 2) is that two Mg^{2+} ions (or two classes of magnesium binding sites) bind completely cooperatively to the E·tRNA complex. The dependence of P RNA affinity for tRNA on the concentration of $MgCl_2$ (Figure 4A) was fit using eq 12 derived for this model, yielding K_1, K_3, and

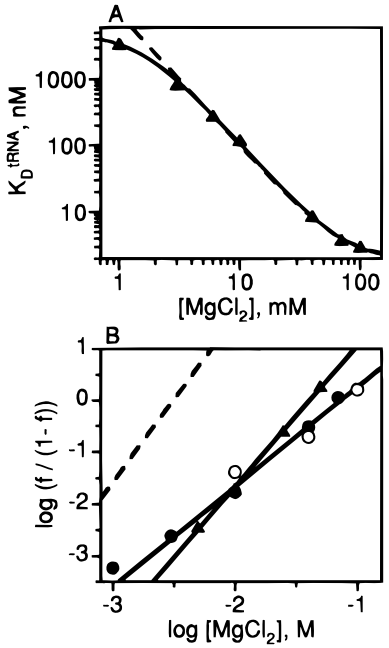

FIGURE 4: (A) Dissociation constants for RNase P RNA and $tRNA^{Asp}$ as a function of $MgCl_2$ concentration. A weighted fit of the data with eq 12 (solid line) yields the equilibrium constants shown in Scheme 2. When the dissociation constant for the E·tRNA complex in the absence of Mg^{2+} (K_1, Scheme 2) is set at 180 μM (dashed line), $K_4 = 0.05 \pm 0.01$ mM, $K_2 = 5000 \pm 1000$ mM, and $K_3 = 2$ nM. (B) Hill plot illustrating the cooperativity of the magnesium dependence for the following: K_D^{tRNA} (●), slope $= 1.9 \pm 0.1$ (Figure 3, minimum $K_D^{tRNA} = 2$ nM); k_{off}^{tRNA} (○), slope $= 1.8 \pm 0.1$ (Figure 5, minimum $k_{off} = 0.008$ s^{-1}); k_{cat}/K_M (▲), slope $= 2.7 \pm 0.1$ (Figure 7, maximum $k_{cat}/K_M = 1 \times 10^6$ M^{-1} s^{-1}); and K_{fold} (dotted line), slope $= 3.2$ [taken from Pan (1995)].

Scheme 2

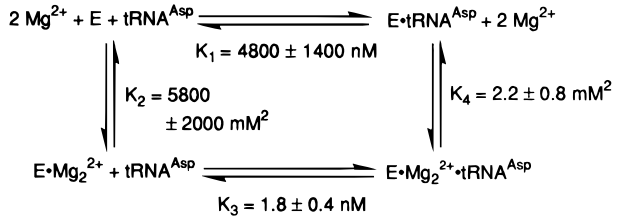

K_4 (Scheme 2).

$$K_{D_{obs}} = K_1(1 + [Mg^{2+}]^2/K_2)/(1 + [Mg^{2+}]^2/K_4) \quad (12)$$

K_3, calculated from $K_3K_2/K_4 = 1.8$ nM to complete the thermodynamic cycle, represents the affinity of P RNA for $tRNA^{Asp}$ at saturating magnesium and is only slightly lower than the value of K_D^{tRNA} of 3.0 ± 0.4 nM measured at 100 mM $MgCl_2$. These data suggest that Mg^{2+} binds to the E·tRNA complex with a dissociation constant, $K_D^{Mg} = 2.2 \pm 0.8$ mM^2, that is much tighter than the affinity of these ions for either free P RNA or tRNA ($K_2 = 5800 \pm 2000$ mM^2). Similarly, this fit of the data indicates that the affinity of P RNA for tRNA in the absence of Mg^{2+} is weak ($K_1 = 4.8 \pm 1.4$ μM), although tighter than the $K_D^{tRNA} \geq 180$ μM estimated from the gel shift assay (Figure 3B). This discrepancy may reflect the following. (1) The fit of the data is not particularly sensitive to the value of K_1 as long as it is large; in fact, the fit is not changed significantly if K_1 increases to 180 μM (see Figure 4A) due to a compensatory increase in the affinity of the bound complex for magnesium ($K_4 = 0.05 \pm 0.01$ mM^2). (2) The gel shift assay underestimates complex formation at low $[Mg^{2+}]$ because the dissociation rate constant is extremely large. Models assuming that the magnesium ions bind independently to either E or E·tRNA also simulate the data as long as the affinity of the first magnesium ion is significantly ($>10^3$-fold) weaker than the affinity of the second.

Table 1: Dissociation Constants for RNase P RNA and $tRNA^{Asp}$ [a]

$[NH_4Cl]$, mM	K_D^{tRNA}, nM		
	0 mM $MgCl_2$	10 mM $MgCl_2$	100 mM $MgCl_2$
10	$\gg$1000 (0.01[b])	$\gg$1000 (0.04)	122 ± 21 (0.31)
100	$\gg$1000 (0.10)	$\gg$1000 (0.13)	17 ± 6 (0.40)
$\geq$800	$\gg$1000[c] (1.10)	119 ± 22[d] (1.10)	3.0 ± 0.4[e] (1.10)

[a] At 50 mM Tris-HCl, pH 8.0, the concentrations of $MgCl_2$ and NH_4Cl indicated, and 37 °C. K_D^{tRNA} was measured as described in the legend of Figure 3. [b] Ionic strength is shown in parentheses. [c] <10% bound complex was observed in a gel shift assay (see Figure 4) at 50 mM Tris-HCl (pH 8.0), 1.1 M NH_4Cl, and P RNA up to 20 μM. [d] $[NH_4Cl] = 1.07$ M. [e] $[NH_4Cl] = 800$ mM.

Finally, we measured the magnesium dependence of K_D^{tRNA} at several concentrations of NH_4Cl (Table 1). These two cations have a synergistic effect on the affinity of P RNA for tRNA; molar concentrations of NH_4Cl decrease the concentration of $MgCl_2$ required to get tight binding ($K_D \leq 100$ nM) by more than 10-fold. This decreased dependence on magnesium at high ammonium may suggest that these two cations stabilize a similar tertiary structure and may reflect tighter binding of tRNA to RNase P in the absence of Mg^{2+} (K_1, Scheme 2), tighter binding of Mg^{2+} to the bound complex (K_4), or weaker binding of Mg^{2+} to unbound P RNA or tRNA (K_2). However, NH_4^+ cannot completely replace Mg^{2+}, as indicated by the low affinity at low concentrations of Mg^{2+} (Figures 3 and 4, Table 1). Therefore, the data indicate that two or more sites in the P RNA·tRNA complex specifically bind magnesium to stabilize formation of this complex.

Cation Dependence of the Rate Constant for Dissociation of tRNA. The rate constant for the dissociation of $tRNA^{Asp}$ from a P RNA·tRNA complex was measured using a competition experiment (Beebe & Fierke, 1994) at a variety of conditions (Figure 5). In this technique, dissociation is initiated by mixing the P RNA·[^{32}P]tRNA (E·tRNA*) complex with a large excess of unlabeled tRNA that competes for the binding site after dissociation of labeled tRNA. The concentration of E·tRNA* versus time is monitored by the radioactivity in the eluate of a gel filtration centrifuge column that separates E·tRNA* from tRNA*. When the rate constant for dissociation of tRNA* is much slower than the rate constant for binding tRNA, the observed rate constant for the disappearance of E·tRNA* directly reflects k_{off}. The maximum rate constant observable by this technique is limited by the transit time [<10 s (Beebe & Fierke, 1994)] of the centrifuge column. The measured dissociation rate constant (Figure 5) increases when either the ammonium chloride or the magnesium chloride concentration decreases, even when the ionic strength is constant to maintain the effective concentration of the RNAs (Day & Underwood, 1986). These increases in dissociation rate constants parallel the observed increases in K_D^{tRNA} (Figures 2 and 3; Table 1), suggesting that the majority of the enhancement of binding of $tRNA^{Asp}$ to P RNA caused by $MgCl_2$ or NH_4Cl is due to a decrease in the dissociation rate constant, k_{off}. In fact, the data are coincident in a Hill plot

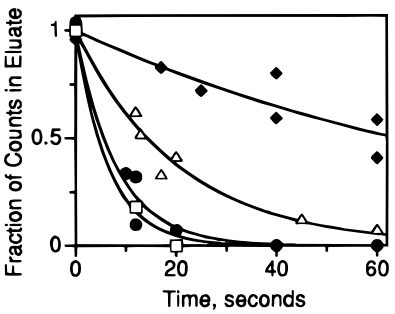

FIGURE 5: Rate constants for the dissociation of tRNA^{Asp} from the E·tRNA complex at various salt concentrations. For each experiment, ^{32}P-labeled tRNA^{Asp} (0.1 nM) was incubated with P RNA (30−1000 nM) for 1 h at 37 °C to form the binary complex. Dissociation of [^{32}P]tRNA^{Asp} was initiated by the addition of excess unlabeled tRNA^{Asp} (0.1−10 μM). The E·[^{32}P]tRNA^{Asp} complex was monitored by the radioactivity in the eluate of a Sephadex G-75 centrifuge column. The fraction of counts in the eluate was calculated from ($cpm_t - cpm_{t_0}$)/($cpm_{t_\infty} - cpm_{t_0}$). The data are fit by a single exponential decay (eq 3); k_{off} values are as follows: 0.013 ± 0.002 s^{-1}, 100 mM $MgCl_2$/800 mM NH_4Cl (◆) [taken from Beebe and Fierke (1994)]; 0.049 ± 0.007 s^{-1}, 40 mM $MgCl_2$/980 mM NH_4Cl (△); 0.10 ± 0.03 s^{-1}, 100 mM $MgCl_2$/80 mM NH_4Cl (●); and ≥0.14 s^{-1}, 10 mM $MgCl_2$/1070 mM NH_4Cl (□).

of the dependence of K_D^{tRNA} or k_{off}^{tRNA} on the concentration of magnesium (Figure 4B). Previous cross-linking data suggested that increasing concentrations of monovalent cations decrease the dissociation rate constant for tRNA^{Phe} (Smith et al., 1992).

The rate constant for association of tRNA with P RNA (k_{on}) can be calculated from the K_D^{tRNA} and k_{off}, assuming a single association step, as 4−6 × 10^6 M^{-1} s^{-1} for varied concentrations of $MgCl_2$ (40 and 100 mM) and NH_4Cl (80 and 980 mM). These values are consistent with the association rate constant of (5.2 ± 0.8) × 10^6 M^{-1} s^{-1} directly measured in 100 mM $MgCl_2$ and 800 mM NH_4Cl (Beebe & Fierke, 1994). To confirm that decreasing the Mg^{2+} concentration 2.5-fold has little effect on the association rate constant, the observed rate constant for the appearance of E·tRNA* was measured after mixing 0.5 nM [^{32}P]tRNA (tRNA*) with 8.6 nM P RNA as 0.10 ± 0.04 s^{-1} (data not shown) using gel filtration centrifuge columns to separate E·tRNA* and tRNA*. The fast half-time of the reaction, $t_{1/2}$ = 7 s, contributes to the error in the experiment. For a simple association reaction, the observed rate constant under pseudo-first-order conditions can be approximated by $k_{obs} = k_{on}$[P RNA] + k_{off}, where k_{on} and k_{off} are the association and dissociation rate constants, respectively. Therefore, the association rate constant can be estimated as ($k_{obs} - k_{off}$)/[P RNA] = (6 ± 3) × 10^6 M^{-1} s^{-1} at 40 mM $MgCl_2$/980 mM NH_4Cl. These data further indicate that the enhancement in binding tRNA^{Asp} to P RNA caused by magnesium is mainly due to a decrease in the dissociation rate constant.

Effect of Magnesium Chloride Concentration on the Steady-State Kinetic Parameters. We have previously demonstrated that product dissociation is the rate-limiting step under k_{cat} conditions at high salt (Beebe & Fierke, 1994). Therefore, the observed dependence of the dissociation rate constant on [Mg^{2+}] (Figure 5) suggests that k_{cat} should decrease at high concentrations of magnesium. To test this, we measured steady-state turnover catalyzed by P RNA as a function of pre-tRNA^{Asp} concentration at lower magnesium concentrations (40 versus 100 mM) (Figure 6). These data display a biphasic dependence on the concentration of pre-

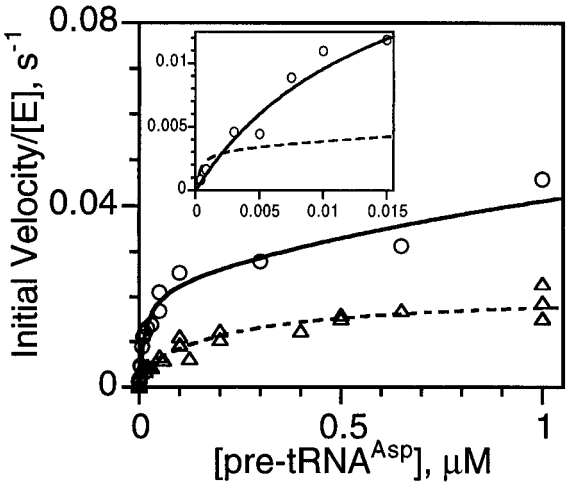

FIGURE 6: Reaction velocity versus pre-tRNA^{Asp} concentration under steady-state conditions. P RNA (2 nM or [S]/[E] ≥ 5 when the substrate concentration was ≤10 nM) was mixed with excess pre-tRNA^{Asp} (0.03−2000 nM) at 37 °C in buffer 1 at the following salt concentrations: 100 mM $MgCl_2$ and 800 mM NH_4Cl (△) (Beebe & Fierke, 1994) and 40 mM $MgCl_2$ and 980 mM NH_4Cl (○). The reactions were quenched by the addition of an equal volume of 200 mM EDTA (pH 8.0)/10 M urea. The initial velocity (<10% hydrolysis) was calculated from the slope of a plot of [tRNA] versus time, and data were fit using eq 4. The inset shows data at substrate concentrations of ≤0.015 μM. Note the biphasic dependence on the concentration of pre-tRNA^{Asp}. The data are fit using eq 4, and the rate constants for the interconversion of E and E′ were estimated by fitting the data after the insertion of all of the other rate constants. At 100 mM $MgCl_2$/800 mM NH_4Cl (dashed line), k_5 = 0.0044 ± 0.001 s^{-1}, and at 40 mM $MgCl_2$/980 mM NH_4Cl, k_5 = 0.037 ± 0.003 s^{-1}.

tRNA^{Asp} and, therefore, cannot be described by the Michaelis−Menten equation (Beebe & Fierke, 1994). However, the observed steady-state data can be fit by eq 4, derived from the scheme shown in Figure 1. In this mechanism, the higher-order dependence on substrate concentration is caused by the slow equilibration between two enzyme conformers (E and E′) that bind pre-tRNA^{Asp} differently. When these data are fit to eq 4 (Figure 6), the initial velocity is defined by the following [rate constants in 100 mM $MgCl_2$ are shown in brackets (Beebe & Fierke, 1994)]: (k_{cat}/K_M)$_1$ = A/C = (1.6 ± 0.4) × 10^6 M^{-1} s^{-1} [5 × 10^6 M^{-1} s^{-1}] measuring the association rate constant of E and S (for S ≤ 10 nM); (k_{cat}/K_M)$_2$ = B/D = (4 ± 2) × 10^4 M^{-1} s^{-1} [7 × 10^4 M^{-1} s^{-1}] representing the binding rate constant of E′ and S (for 10 nM ≤ [S] ≤ 100 nM); and k_{cat} = B/E = 0.086 ± 0.031 s^{-1} [0.02 s^{-1}] reflecting the rate constant for tRNA dissociation ([S] > 2 μM). This value of k_{cat} is within experimental error of the rate constant for tRNA dissociation under these conditions (0.05 s^{-1}), confirming both that product dissociation remains the rate-limiting step for turnover and that increasing concentrations of Mg^{2+} decrease the rate constant for this step. Therefore, very high concentrations of Mg^{2+} actually inhibit steady-state turnover by decreasing the rate constant for tRNA dissociation.

These data also indicate that the rate constant for conversion of E′ to E (k_5) increases as the concentration of magnesium is lowered since a higher substrate concentration is required to produce a change in the rate-limiting step from the association of E and S (when E′ converts to E faster than E′ binds S) to the binding of E′ and S (Figure 6 inset). The interconversion rate constants can be estimated from a fit of the steady-state data using eq 4 with the rate constants

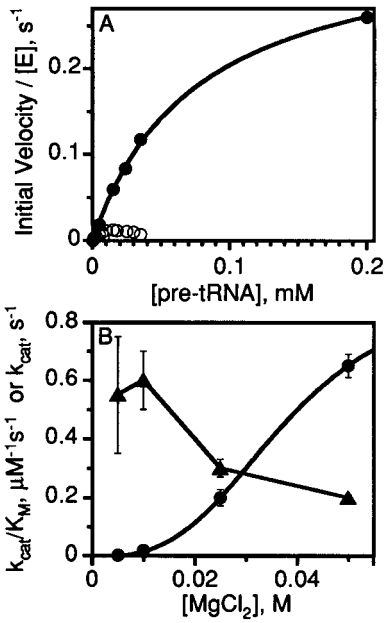

FIGURE 7: Dependence of steady-state kinetic parameters on the concentration of magnesium. (A) P RNA (20−400 nM, prepared in the absence of EDTA) was mixed with excess pre-tRNA^{Asp} (0.2−200 μM) at 37 °C in 50 mM Tris-HCl (pH 8.0), 5 mM $MgCl_2$, and 100 mM NH_4Cl. The P RNA and pre-tRNA^{Asp} were prepared either by dilution into this buffer (○) or by dilution followed by dialysis against a 2000-fold excess volume of the same buffer at 37 °C (●) to ensure that $[MgCl_2]_{free}$ = 5 mM. The reactions were stopped and analyzed as described in the legend of Figure 6. For the reactions dialyzed against buffer, the initial velocity displays a single, hyperbolic dependence on the concentration of pre-tRNA^{Asp} so the data are fit using the Michaelis−Menten equation, k_{cat} = 0.55 ± 0.2 s^{-1} and $k_{cat}/K_M = (3.5 \pm 0.5) \times 10^3$ M^{-1} s^{-1}; however, the data using solutions that have not been dialyzed are less well-described by a hyperbolic function since the initial velocity decreases at high [pre-tRNA^{Asp}]. Dialysis increases k_{cat} without greatly affecting k_{cat}/K_M. (B) The substrate dependence of the initial velocity for RNase P-catalyzed cleavage of pre-tRNA^{Asp} was measured as a function of the concentration of $MgCl_2$ (5−50 mM), and the steady-state kinetic parameters, k_{cat}/K_M (●) and k_{cat} (▲), were calculated by fitting the data as described in part A. Above 10 mM $MgCl_2$, dialysis of the substrate against buffer had little effect on the kinetic parameters. The k_{cat}/K_M data were fit (eq 9) assuming that the exponential dependence on magnesium, as indicated by the Hill coefficient (Figure 4), is 3. At low magnesium, k_{cat} becomes slower than k_{off}, likely due to a change in the rate-limiting step in k_{cat}.

defined in the kinetic scheme (Figure 1), except for $k_1 = 2 \times 10^6$ M^{-1} s^{-1} determined from pre-steady-state experiments, $k_6 = 4 \times 10^4$ M^{-1} s^{-1} estimated from $(k_{cat}/K_M)_2$; $k_4 = 0.05$ s^{-1} measured directly (Figure 5 and 6); and $k_{-1} = 2$ s^{-1} estimated as an increase in the dissociation rate constant of pre-tRNA^{Asp} proportional to that of k_{off}^{tRNA}. A value for k_5 = 0.04 ± 0.01 s^{-1} resulted, and the fit was insensitive to the value of k_{-5}/k_5 as long as it was ≤0.5. This indicates that the rate constant for conversion of E′ to E increases as the $[MgCl_2]$ decreases, suggesting that bound magnesium ion(s) stabilize E′ (and perhaps E as well) relative to the transition state for the conformational change.

At lower concentrations of magnesium and ammonium chloride, the concentration dependence of steady-state turnover can be described by the Michaelis−Menten equation (Figure 7A) since the higher-order dependence on substrate concentration disappears as the rate constant for interconversion between the two enzyme conformers increases. Furthermore, at 5 mM $MgCl_2$, the observed steady-state k_{cat} and K_M increase more than 100-fold if the substrate is dialyzed against buffer containing 5 mM magnesium (Figure 7A). This indicates that the high concentrations of RNA required for catalysis under these conditions bind a significant fraction of the total magnesium concentration to deplete the concentration of free magnesium; dialysis maintains $[Mg^{2+}]$ at 5 mM. The stoichiometry of magnesium binding to tRNA and P RNA is approximately one Mg^{2+} per four nucleotides, similar to the stoichiometry for the binding of Mn^{2+} to yeast tRNA^{Phe} (Schreir & Schimmel, 1974; see Figure 9). This result may also explain the previously observed low activity of P RNA at low concentrations of magnesium (Guerrier-Takada et al., 1983, 1986).

As the concentration of magnesium decreases, the second-order rate constant, k_{cat}/K_M, decreases significantly while both k_{cat} and K_M increase (Figure 7B). The increase in k_{cat} is predicted by the increase in the dissociation rate constant for tRNA, the rate-limiting step in steady-state turnover, and the increase in K_M parallels the increase in K_D (Figures 3A and 4). A Hill plot of the dependence of k_{cat}/K_M on magnesium concentration (Figure 4B) has a slope of 2.7 ± 0.1, suggesting that three magnesium or types of magnesium ion binding sites are required for stabilization of the catalytic transition state compared to unbound substrates. These data are consistent with the magnesium dependence of single-turnover k_{cat}/K_M for hydrolysis of pre-tRNA^{Phe} by *E. coli* RNase P RNA at pH 6 (Smith & Pace, 1993).

Effects of Magnesium Concentration on Binding and Catalysis as Measured by Single-Turnover Experiments. The pre-tRNA association and the hydrolytic cleavage steps catalyzed by P RNA can be isolated by measuring a single turnover in the presence of excess enzyme ([E]/[S] ≥ 5) (Beebe & Fierke, 1994). Under these conditions, product dissociation is not observable since E·tRNA and tRNA are indistinguishable on denaturing polyacrylamide gels. Therefore, to further examine the role of Mg^{2+} on binding and catalysis, single-turnover experiments were performed at decreased concentrations of Mg^{2+} and constant ionic strength at both low (121 nM) and high (19 μM) concentrations of P RNA. At low [P RNA] (Figure 8A), the data are well-fit by a single pseudo-first-order exponential (eq 5) and the observed rate constants are dependent on the concentration of P RNA (data not shown). The calculated second-order rate constant for hydrolysis of pre-tRNA^{Asp} is $(3.3 \pm 0.1) \times 10^6$ M^{-1} s^{-1} (100 mM $MgCl_2$), $(2.4 \pm 0.2) \times 10^6$ M^{-1} s^{-1} (40 mM $MgCl_2$), and $(0.6 \pm 0.1) \times 10^6$ M^{-1} s^{-1} (10 mM $MgCl_2$). This observed decrease at low magnesium indicates that either the association rate constant decreases (if $k_2 > k_{-1}$) or a change in the rate-limiting step occurs (if $k_2 < k_{-1}$) so that $k_{obs} \approx k_1k_2/k_{-1}$. In fact, the observed decrease in the association rate constant at 10 mM $MgCl_2$ could be explained by a 3.7-fold decrease in k_2 (see Figure 8B) combined with a 14-fold increase in k_{-1} so that $k_{-1} > k_2$. This proposed increase in the dissociation rate constant for pre-tRNA^{Asp} is consistent with the >10-fold increase in the dissociation rate constant observed for tRNA^{Asp} (Figure 5) under similar conditions.

For single-turnover experiments at high P RNA concentrations (Figure 8B) where cleavage is rate-limiting, data were fit to an equation for two consecutive first-order reactions (eq 6); the cleavage rate constant decreases only modestly, k_2 = 5.9 ± 0.3 versus 4.6 ± 0.2 s^{-1}, when the $[MgCl_2]$ decreases from 100 to 40 mM. At 10 mM $MgCl_2$, data were

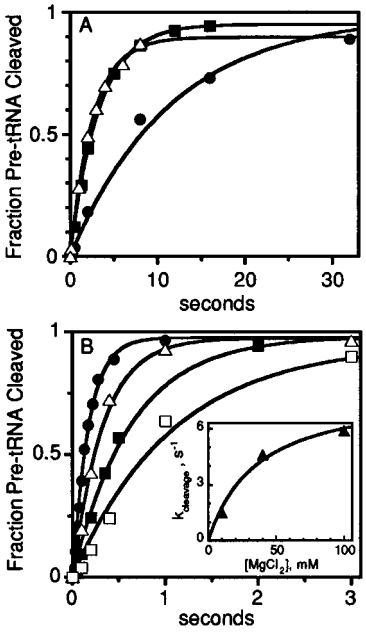

FIGURE 8: Single-turnover measurements of RNase P RNA-catalyzed hydrolysis of pre-tRNA^{Asp} performed at various concentrations of $MgCl_2$ while the ionic strength was maintained using NH_4Cl. (A) Pre-tRNA^{Asp} (12−24 nM) was mixed with 121 nM P RNA, reactions were quenched with EDTA, and products were separated by polyacrylamide gel electrophoresis and quantified using a PhosphorImager. Data were fit by a single exponential (eq 5), with the following results: 100 mM $MgCl_2$/800 mM NH_4Cl, $k_{obs} = 0.38 \pm 0.02$ s^{-1} (△) [taken from Beebe and Fierke (1994)]; 40 mM $MgCl_2$/980 mM NH_4Cl, $k_{obs} = 0.31 \pm 0.01$ s^{-1} (■); and 10 mM $MgCl_2$/1070 mM NH_4Cl, $k_{obs} = 0.09 \pm 0.02$ s^{-1} (●). (B) Pre-tRNA^{Asp} (0.012−0.024 μM) was mixed with P RNA (2.4−19 μM), reactions were quenched with EDTA, and products were separated by polyacrylamide gel electrophoresis and quantified using a PhosphorImager. Data at high concentrations of $MgCl_2$ were fit with an equation for a double exponential (eq 6) using $k_1 = 6 \times 10^6$ M^{-1} s^{-1} with the following results: 100 mM $MgCl_2$/800 mM NH_4Cl ([S] = 0.024 μM, [E] = 19 μM), $k_{obs} = 5.9 \pm 0.3$ s^{-1} (●) [taken from Beebe and Fierke (1994)]; and 40 mM $MgCl_2$/980 mM NH_4Cl ([S] = 0.012 μM, [E] = 2.4 μM), $k_{obs} = 4.6 \pm 0.2$ s^{-1} (△). At 10 mM $MgCl_2$/1070 mM NH_4Cl ([S] = 0.012 μM), data were fit to the equation for a single exponential (eq 5), yielding the following: $k_{obs} = 1.6 \pm 0.1$ s^{-1} at [E] = 15 μM (■) and $k_{obs} = 0.9 \pm 0.1$ s^{-1} at [E] = 2.4 μM (□). (inset) The hydrolytic rate constant is plotted versus the $MgCl_2$ concentration; a hyperbolic fit of the data indicates a maximum cleavage rate constant of $k_{cleavage} = k_2 = 8.2 \pm 1.2$ s^{-1} and $K_{Mg} = 36 \pm 14$ mM.

fit to the equation for a single exponential (eq 1) since $k_{-1} > k_2$, yielding $k_2 = 1.6 \pm 0.1$ s^{-1} which is decreased 3.7-fold compared to the cleavage rate constant at 100 mM $MgCl_2$. Furthermore, these rate constants are not dependent on the concentration of P RNA (Figure 8B; Beebe & Fierke, 1994), indicating that they are measuring the maximal rate constant for cleavage under these conditions. The hydrolytic rate constant has a hyperbolic dependence on the concentration of magnesium with a maximum rate constant extrapolating to $k_2 = 8.2 \pm 1.2$ s^{-1} and an apparent $K_{Mg} = 36 \pm 14$ mM (Figure 8B). These data suggest that there is one weak magnesium binding site in the E·S complex that increases the hydrolytic rate constant.

Measurement of the Binding of Magnesium to RNase P RNA. To further investigate the interaction between magnesium and P RNA, both the number of magnesium ions that bind to P RNA and the dissociation constant for these ions were measured using a gel filtration centrifuge column to separate bound and free magnesium. This column

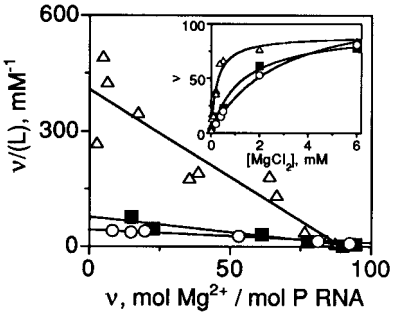

FIGURE 9: Binding of Mg^{2+} to RNase P RNA as measured by the separation of bound and free Mg^{2+} via centrifuge columns, followed by quantitation of bound Mg^{2+} in the eluate by a hydroxyquinoline fluorescence detection assay. P RNA (3 μM) was incubated in buffer 1 at specified concentrations of $MgCl_2$ and NH_4Cl for 15 min at 37 °C. Data were fit using eq 8, the equation for a Scatchard plot. Concentrations of NH_4Cl were 1.1 M (○), 0.8 M (■), and 0 (△). In order to clearly present the large amount of data, an inset showing direct fits of data (eq 7) in which [NH_4Cl] = 1.1 M (○), 0.8 M (■), and 0.1 M (△) is presented. Results are summarized in Table 2.

Table 2: Binding of Magnesium to RNase P RNA[a]

[NH_4Cl], M	n[b]	K_D, mM	α_H[c]	slope[d]
1.1	125 ± 10	2.8 ± 0.3	0.92 ± 0.04	−1.07 ± 0.04
0.8	93 ± 6	1.2 ± 0.1	1.1 ± 0.1	−0.89 ± 0.08
0.1	95 ± 6	0.39 ± 0.08	1.1 ± 0.1	−0.8 ± 0.1
0.0	89 ± 4	0.21 ± 0.02	0.98 ± 0.05	−1.0 ± 0.05

[a] Conditions: 50 mM Tris-HCl, pH 8.0, and 37 °C. Mg^{2+} was separated from P RNA·Mg^{2+} using centrifuge columns followed by quantitation of bound Mg^{2+} using a fluorescence detection assay as described in Materials and Methods. [b] n = number of Mg^{2+} binding sites. [c] α_H = Hill constant. [d] Slope = $-1/\alpha_H$ (see eq 10, Materials and Methods).

efficiently retains magnesium in the gel matrix; after the addition of 30 μL of buffer 1 containing 100 mM $MgCl_2$ to a 600 μL Sephadex G-50 column followed by centrifugation, 0.3 nmol (10 μM in a 30 μL volume, 10 000-fold less concentrated than buffer 1) of magnesium was observed in the eluate. This would produce a value of $n = 3$ in an experiment using 3 μM P RNA. Background values decreased at lower concentrations of $MgCl_2$ and were subtracted from the data. The amount of magnesium observed in the eluate is linearly dependent on the concentration of P RNA (3−10 μM) and also varies with the concentration of $MgCl_2$ and NH_4Cl. The concentration of magnesium in the eluate is determined by the observed fluorescence compared to a standard curve after the addition of 8-hydroxyquinoline-5-sulfonic acid to produce the fluorescent complex magnesium−8-quinolinol (Watanabe et al., 1963; Niranjanakumari and Fierke, unpublished data). In order to clearly present all data, both linearized and direct fits are shown (Figure 9). These data can be fit assuming multiple, independent binding sites; Hill coefficients of approximately 1 have been determined for all data (eq 9, Table 2), demonstrating a lack of cooperativity. However, a small number of high-affinity sites (<10) would not be observable with this technique. Under all conditions, a large number of magnesium ions bind to RNA, 90−130 mol of Mg^{2+} per mole of RNase P for an average of about one Mg^{2+} per four nucleotides. To check the accuracy of the maximal number of bound magnesium ions, the data were also fit using eq 10 since the linearity of this plot is very sensitive to the value of n (Cantor & Schimmel, 1980). In these plots,

the data are linear with a slope of $-1/\alpha_H$ (where α_H = Hill constant). The number of magnesium binding sites and the dissociation constants are listed in Table 2. These values are comparable to the affinity and stoichiometry of manganese binding to yeast $tRNA^{Phe}$ measured by equilibrium dialysis (Schreier & Schimmel, 1974).

Equilibrium dialysis experiments (Bell & Bell, 1988) were carried out to confirm the effectiveness of the gel filtration centrifuge columns in separating free and bound magnesium (described in Materials and Methods). Two trials were performed in 50 mM Tris-HCl (pH 8) at 0.3 mM $MgCl_2$ and 4.5 μM P RNA, resulting in values of L_{free} = 0.18 and 0.17 mM, E_{free} = 2.8 and 2.7 μM, and [E·L] = 2.0 and 1.4 μM. Using eq 1, dissociation constants of 0.25 and 0.33 mM (average = 0.3 ± 0.1 mM) were calculated assuming a value of n = 89. These dissociation constants are similar to that measured using centrifuge columns (0.21 ± 0.02 mM, see Figure 9 and Table 2).

As the concentration of NH_4Cl increases, the K_D^{Mg} also increases but the total number of magnesium binding sites remains relatively constant. A Hill plot of these data (not shown) has a slope of 1 ± 0.2, indicating a noncooperative dependence of K_D^{Mg} on NH_4Cl. These data suggest that NH_4Cl competes with $MgCl_2$, either directly by binding to the magnesium sites or indirectly by decreasing the electrostatic interaction between Mg^{2+} and the negatively charged RNA.

DISCUSSION

Binding of Mg^{2+} to RNase P RNA. Quantitation of the number of Mg^{2+} ions bound to P RNA indicates a stoichiometry of about 100 ions that bind independently with a dissociation constant of 0.2−3 mM, depending on the NH_4Cl concentration (Figure 9, Table 2). This stoichiometry is comparable to previous measurements for other RNAs. For example, yeast $tRNA^{Phe}$ contains 25 ± 3 sites for binding Mn^{2+} (Schreier & Schimmel, 1974); five of these Mn^{2+} sites are associated with a cooperative phase, twelve sites are independent and possess a dissociation constant of 0.016 mM, and the eight weak sites have a dissociation constant estimated at 1.4 mM. In general, ions of opposite charge cluster close to the surface of highly charged polyelectrolytes (such as nucleic acids) due to the strong Coulombic field, designated counterion condensation [see reviews in Manning (1978, 1979), and Anderson and Record (1990, 1995)]. Counterions surrounding a charged polyanion may either be immobilized at a specific site or nonspecifically associated due to electrostatic interactions. The fraction of counterions thermodynamically associated with DNA/phosphate is a function of the axial charge density on the nucleic acid. For B DNA, the calculated fraction of condensed counterions is 0.76 M^+/phosphate and 0.44 M^{2+}/phosphate. The observed stoichiometry of Mg^{2+} binding to P RNA is smaller than this value, ≈0.25 Mg^{2+}/phosphate (Figure 9, Table 2), but consistent with the majority of these ions being electrostatically associated. The decreased stoichiometry could be due to either a significant decrease in the linear charge density of P RNA compared to that of B DNA or to equilibration of magnesium ions with other cations during the transit time of the gel filtration spin columns. The dependence of the dissociation constant, but not the stoichiometry, on the concentration of ammonium chloride suggests that NH_4^+ competes with Mg^{2+} in condensing with RNase P RNA (Table 2). A similar competition between monovalent and multivalent counterions has previously been observed for B DNA (Record et al., 1976; Lohman et al., 1980). The independent nature of the magnesium binding sites in P RNA is consistent with the nonspecific nature of the interaction of condensed cations with P RNA. This result is significantly different from the cooperative dependence of P RNA folding (Pan, 1995) or tRNA binding (Figure 4) on magnesium concentration presumably due to specific binding sites. However, a few cooperative magnesium binding sites (<10) would not be observable in the background of a large number of independent sites. These data demonstrate that a large number of magnesium ions are electrostatically associated with the highly negatively charged P RNA to neutralize the charge. Additional magnesium ions may bind to P RNA in a site-specific fashion, and these ions likely play multiple functional roles.

One role for metal ions, especially divalent ones such as Mg^{2+}, is the stabilization of the structure of many types of RNA, including tRNA (Crothers, 1979), the *Tetrahymena* ribozyme (Wang & Cech, 1994; Zarrinkar & Williamson, 1994), and *B. subtilis* P RNA (Pan, 1995). Folding of P RNA, as assayed by Fe(II)−EDTA protection, is cooperative with a Hill coefficient of about 3 and a transition midpoint of 2−3 mM in the presence of 0−0.1 M KCl (Pan, 1995). Under these conditions, the measured dissociation constant for magnesium, 0.2−0.4 mM (Table 2), is lower than the folding transition midpoint, indicating that the majority of magnesium ions are electrostatically associated with "unfolded" P RNA while a minority of sites are important for specific stabilization of the folded structure.

Requirement for Metal Ions in the Binding of RNase P RNA and tRNA. Our data indicate that a second role for magnesium binding to P RNA is to increase the affinity of *B. subtilis* RNase P RNA for *B. subtilis* $tRNA^{Asp}$. In fact, K_D^{tRNA} is completely and cooperatively dependent on magnesium, even at concentrations where P RNA is completely folded (Figures 3 and 4; Pan, 1995), suggesting that binding two additional magnesium ions or classes of ions is essential for the formation of the P RNA·tRNA complex. Furthermore, the addition of other salts, such as NH_4Cl, does not eliminate this requirement, indicating that magnesium interacts specifically with the bound complex, rather than simply neutralizing negative charge. The binding of Mg^{2+} to the P RNA·tRNA complex may promote high affinity either indirectly by causing structural changes in P RNA or $tRNA^{Asp}$ in this complex and/or directly by the formation of specific salt bridges between the two molecules. If these additional magnesium ion sites occur near the cleavage site, they may also play a role in catalysis of the cleavage step.

The affinity of P RNA for tRNA increases at concentrations of magnesium well above the measured K_D for magnesium (1−3 mM; Figure 9, Table 2) and the $[Mg^{2+}]_{1/2}$ for folding P RNA (Pan, 1995) with the midpoint of the enhanced affinity for tRNA occurring at 75 mM $MgCl_2$ (Figure 4). This high concentration of magnesium reflects the coupling between the binding of magnesium and tRNA to P RNA; these magnesium binding sites are low-affinity sites in the unbound complex (5500 mM^2) but are much stronger in the P RNA·tRNA complex where $K_D \approx 2$ mM^2 (Scheme 2). Therefore, the magnesium dependence of K_D^{tRNA} does not directly measure the affinity of the magne-

sium sites in the E·Mg^{2+} binary complex.

Additionally, monovalent cations have opposing effects on the affinity of P RNA for Mg^{2+} and tRNA; K_D^{tRNA} decreases at higher NH_4Cl with a midpoint at 6 mM NH_4Cl (Figure 2), while K_D^{Mg} increases at higher NH_4Cl (Figure 9, Table 2). Ammonium chloride does not increase the affinity of tRNA by enhancing the affinity of magnesium to P RNA, nor does the data in Table 2 suggest that ammonium chloride promotes Mg^{2+} binding to the P RNA·tRNA complex. Therefore, saturation of P RNA with Mg^{2+} is not the only mechanism for enhancing the affinity of P RNA for tRNA. Additional cations likely provide electrostatic shielding within or between the RNAs, but in a more site-specific manner than simple electrostatic shielding in solution. Monovalent cations such as NH_4^+, Cs^+, K^+, or Rb^+ (Smith et al., 1992) play an important role in promoting tight binding between P RNA and tRNA that is not identical to the requirement for Mg^{2+}. Ammonium ions stabilize the P RNA·tRNA complex relative to the unbound species, perhaps by binding to additional high-affinity binding sites in the binary complex, as shown in Scheme 1, or by decreasing the affinity of magnesium sites in P RNA.

In a previous study, monovalent cations were found to be sufficient to support binding between *B. subtilis*, *E. coli*, or *Chromatium vinosum* RNase P RNA and yeast or *E. coli* azidophenacyl-$tRNA^{Phe}$ as assayed by cross-linking (Smith et al., 1992). *B. subtilis*, *E. coli* and *C. vinosum* RNase P RNA exhibited only a 7-, 3-, or 1.1-fold, decrease, respectively, in cross-linking with *E. coli* $tRNA^{Phe}$ in the absence of magnesium. Possible reasons for the discrepancy between centrifuge column and gel shift experiments versus the cross-linking data include the following. (i) Sequence differences between azidophenacyl-$tRNA^{Phe}$ and $tRNA^{Asp}$ may influence the magnesium dependence of tRNA affinity. (ii) The amount of binding between P RNA and tRNA as assayed by cross-linking could be overestimated if cross-linking of the low concentration of P RNA·tRNA is rapid and coupled to rapid equilibration between bound and free enzyme. (iii) Structural differences between various RNase P RNAs may influence the dependence of tRNA binding on Mg^{2+}. Although bacterial RNase P RNAs contain a core of homologous sequence and structure, secondary structure of *B. subtilis* P RNA differs significantly from that of *E. coli* [Haas et al., 1991, 1994; La Grandeur et al., 1994; reviewed in Pace and Brown (1995)]. For example, the pseudoknot that forms helix P6 is present in all forms of bacteria examined except the low-G+C subdivision, of which *B. subtilis* is a member. However, helix P5.1 is unique to the low-G+C subdivision and possesses a three-dimensional structure resembling that of helix P6. These structural differences may affect the magnesium and tRNA affinity of RNase P RNA.

Cations Decrease the Rate Constant for $tRNA^{Asp}$ Dissociation and the Efficiency of P RNA-Catalyzed Turnover. The increased affinity of P RNA for $tRNA^{Asp}$ at high concentrations of magnesium and ammonium chloride is due to a decrease in the rate constant for dissociation (k_{off}) of $tRNA^{Asp}$ from the P RNA binary complex, while the association rate constant (k_{on}) is unaffected (Figures 4 and 5). Under these conditions (10−100 mM $MgCl_2$), P RNA is folded (Pan, 1995). Mechanisms involving a rate-limiting step for association of P RNA and tRNA preceding the binding of ammonium or magnesium to the E·tRNA complex are

Scheme 3

$$E + tRNA^{Asp} \underset{k_{-1}}{\overset{k_1}{\rightleftharpoons}} E{\cdot}tRNA^{Asp} + 2\,Mg^{2+} \underset{k_{-2}}{\overset{k_2}{\rightleftharpoons}} E{\cdot}tRNA^{Asp}{\cdot}2Mg^{2+}$$

consistent with the effects of these cations on k_{off} and k_{on}. For example, the simplest mechanism (Scheme 3) involves the rate-limiting association of P RNA and $tRNA^{Asp}$ prior to the binding of two Mg^{2+} ions or classes of ions (Figures 3 and 4, Scheme 2). For this mechanism, k_{on} is independent of $[Mg]^{2+}$ and k_{off} is inversely proportional to the square of $[Mg^{2+}]$ (as shown in eqs 13 and 14 derived using the steady-state assumption under irreversible conditions) if $k_2[Mg^{2+}]^2 > k_{-1}$. Additionally, the steady-state and pre-steady-state data suggest that the magnesium dependence of the association and dissociation rate constants for pre-$tRNA^{Asp}$ is similar to that of $tRNA^{Asp}$.

$$k_{on} = k_1[E]k_2[Mg^{2+}]^2/(k_1[E] + k_{-1} + k_2[Mg^{2+}]^2)$$

$$\approx k_1[E] \quad \text{if } k_2[Mg^{2+}]^2 > k_{-1} + k_1[E] \tag{13}$$

$$k_{off} = k_{-1}k_{-2}/(k_{-1} + k_{-2} + k_2[Mg^{2+}]^2)$$

$$\approx k_{-1}k_{-2}/k_2[Mg^{2+}]^2 \quad \text{if } k_2[Mg^{2+}]^2 > k_{-1} + k_{-2} \tag{14}$$

Steady-state turnover (k_{cat}) catalyzed by P RNA increases as the concentration of either $MgCl_2$ or NH_4Cl decreases (Figures 6 and 7) since the rate constant for dissociation of $tRNA^{Asp}$ is the rate-limiting step at high cation concentrations (Beebe & Fierke, 1994). Furthermore, product inhibition is pronounced because K_D^{tRNA} is lower than the dissociation constant for pre-tRNA. (However, product inhibition is attenuated by the formation of E′ since this form of the enzyme has lower affinity for both products and substrates.) The magnesium dependence of k_{off} and $k_{cleavage}$ (Figures 5 and 8) suggest that the cleavage rate constant should become the rate-limiting step in steady-state turnover at ≈5 mM $MgCl_2$ in the presence of 800 mM NH_4Cl and k_{cat} should then decrease at lower concentrations of Mg^{2+}. At high concentrations of $MgCl_2$ and NH_4Cl, k_{cat}/K_M is not dependent on the concentration of Mg^{2+} (Figure 6) because substrate association is the rate-limiting step at low pre-$tRNA^{Asp}$ concentrations. Differences in the cation dependence of steady-state cleavage of various RNA substrates by P RNA (Green & Vold, 1988; Roselli & Marsh, 1990) may reflect a change in the rate-limiting step since the association, cleavage, and dissociation steps have differential dependence on cations. At physiological concentrations of magnesium and ammonium, P RNA has a low catalytic efficiency caused mainly by the low affinity for pre-$tRNA^{Asp}$ (K_D > 1 μM).

Mg^{2+} Stabilizes the Transition State for Cleavage. The magnesium dependence of the single-turnover rate constant for pre-$tRNA^{Asp}$ cleavage at saturating P RNA (Figure 8) revealed that the cleavage rate constant has a hyperbolic dependence on magnesium chloride with $K_{1/2} \approx 36$ mM. Therefore, a third low-affinity magnesium binding site in the P RNA·pre-$tRNA^{Asp}$ complex participates in catalysis either directly by interacting with the transition state or indirectly by influencing the conformation of the bound complex. Previous mechanisms for RNase P-catalyzed cleavage of pre-tRNA have suggested catalytic roles for one

to three magnesium ions (Haydock & Allen, 1985; Guerrier-Takada et al., 1986; Smith & Pace, 1993; Steitz & Steitz, 1993). Our data provide evidence for the catalytic participation of one magnesium ion; however, this does not preclude the involvement of additional ions such as the magnesium ions that stabilize the binding of tRNA. Divalent metal ions may be involved in the catalytic step [reviewed in Pyle (1993) and Smith (1995)] by acting as a general acid or general base, as suggested for the hammerhead ribozyme (Dahm et al., 1993); stabilizing the leaving group (Sugimoto et al., 1988; Beese & Steitz, 1991; Piccirilli et al., 1993); destabilizing the ground state by interacting with a bridging phosphate oxygen bond at the cleavage site (Narlikar et al., 1995); and/or stabilizing an oxyanion in the transition state (Dahm & Uhlenbeck, 1991).

Metal cofactors have been proposed to play a number of crucial roles in ribozymes. In *B. subtilis* P RNA, the roles of bound magnesium can be separated functionally into three categories: at least three sites stabilize RNA folding (Pan, 1995), at least two sites are required for binding pre-tRNA and tRNA, and at least one site catalyzes the cleavage of pre-tRNA. [Therefore, a total of at least three magnesium binding sites is reflected in k_{cat}/K_M (Figure 4), consistent with the results of Smith and Pace (1992).] In each case, these functional assays reflect magnesium ions that bind to either the folded state or the binary complex preferentially. Given the large number of magnesium ions that interact with P RNA (Figure 9, Table 2), it is likely that the majority of magnesium ions bind to both states similarly, consistent with the nonspecific interactions of condensed counterions [see reviews in Manning (1978, 1979) and Anderson and Record (1990, 1995)], and/or that the Hill coefficients reflect the number of types of independent binding sites rather than the actual number of sites.[2]

Crystal structures of tRNA indicate that Mg^{2+} binds as an octahedrally coordinated species, either as a hexaaquo complex with hydrogen bonding between water molecules within the hydration sphere and tRNA bases or phosphoryl groups or with replacement of one or two of the water molecules by direct coordination to phosphoryl oxygens (Holbrook et al., 1977; Quigley et al., 1978; Smith, 1995). One Mg^{2+} binding site in the enzyme−substrate complex has been proposed to interact with the 2′-OH of the cleaved phosphodiester bond since removal of this OH significantly decreases the cleavage rate constant (Smith & Pace, 1993). Similarly, other 2′-modified ribose moieties near the cleavage site (positions −2, −1, and +1) interfere with RNase P-catalyzed cleavage, perhaps suggesting additional magnesium binding sites in this region (Kleinedam et al., 1993; Perreault & Altman, 1992). Additionally, phosphorothioate modification−interference experiments have identified four phosphate oxygens in *E. coli* P RNA where substitution by sulfur significantly reduces both the rate constant for self-cleavage of a P RNA−substrate conjugate (Harris & Pace, 1995) and the affinity of P RNA for tRNA (Hardt et al., 1995). These sites are immediately adjacent to the cleavage site in a low-resolution structural model of *E. coli* P RNA (Harris et al., 1994). Modification−interference studies have also implicated additional phosphoryl oxygens important for tRNA affinity (Hardt et al., 1995). Furthermore, several sites were partially rescued in the presence of manganese, suggesting a direct involvement in binding divalent metal ions. Investigation of the effect of specific 2′-deoxy or phosphorothioate substitution on the three functional assays for magnesium binding sites in *B. subtilis* P RNA may further identify the position(s) of the magnesium sites crucial for catalysis and substrate affinity.

Role of the Protein Component. The RNase P holoenzyme has a significantly higher k_{cat}/K_M at low concentrations of magnesium compared to the P RNA (Reich et al., 1988), likely due mainly to an increased affinity for pre-tRNA (Tallsjö & Kirsebom, 1993; Kurz and Fierke, unpublished data). If the protein component mimics the effect of high concentrations of magnesium, this increased affinity should be accompanied by a decreased dissociation rate constant and a lower k_{cat}. However, the protein component increases k_{cat} ≤2-fold at a constant cation concentration (Tallsjö & Kirsebom, 1993; Niranjanakumari, Kurz, and Fierke, unpublished data), indicating that this is not the main function of the protein. If the protein increases the affinity of P RNA for products and substrates without decreasing the dissociation rate constant, then the observed association rate constant must increase. Therefore, these data suggest that a main role of the protein component is to increase the association rate constant for pre-tRNA by increasing the concentration of RNase P with the correct tertiary structure and bound magnesium ions. We previously hypothesized that the protein might prevent the formation of a less active conformer, E′ (Beebe & Fierke, 1994); however, our current data indicate that conversion of E′ to E is fast at low magnesium concentrations (Figure 6) so the protein is not required to facilitate this step. Additionally, a role for the protein component in the chemical step or increasing the affinity of the catalytic magnesium ion has not been ruled out.

ACKNOWLEDGMENT

We thank Drs. Michael Been, Niranjanakumari, and Dan Herschlag for providing helpful advice. We also thank Dr. Norman Pace for giving us useful plasmids.

REFERENCES

Altman, S. (1989) *Adv. Enzymol. 62*, 1−36.
Anderson, C. F., & Record, M. T., Jr. (1990) *Annu. Rev. Biophys. Biophys. Chem. 19*, 423−465.
Anderson, C. F., & Record, M. T., Jr. (1995) *Annu. Rev. Phys. Chem. 46*, 657−700.
Baer, M. F., Wesolowski, D., & Altman, S. (1989) *J. Bacteriol. 171*, 6862−6866.
Beebe, J. A., & Fierke, C. A. (1994) *Biochemistry 33*, 10294−10304.
Beese, L. S., & Steitz, T. A. (1991) *EMBO J. 10*, 25−33.
Bell, J. E., & Bell, E. T. (1988) in *Proteins and Enzymes*, pp 379−381, Prentice-Hall, Inc., Englewood Cliffs, NJ.
Bujalowski, W., Graeser, E., McLaughlin, L. W., & Porschke, D. (1986) *Biochemistry 25*, 6365−6371.
Cantor, C. R., & Schimmel, P. R. (1980) in *Biophysical Chemistry*, pp 850−866, W. H. Freeman and Company, New York.
Celander, D. W., & Cech, T. R. (1991) *Science 251*, 401−407.
Crothers, D. M. (1979) in *Transfer RNA: Structure, Properties, and Recognition*, pp 163−176, Cold Spring Harbor Laboratory Press, Plainview, NY.
Dahm, S. C., & Uhlenbeck, O. C. (1991) *Biochemistry 30*, 9464−9469.
Dahm, S. C., Derrick, W. B., & Uhlenbeck, O. C. (1993) *Biochemistry 32*, 13040−13045.
Davanloo, P., Rosenberg, A. H., Dunn, J. J., & Studier, F. W. (1984) *Proc. Natl. Acad. Sci. U.S.A. 81*, 2035−2039.
Day, R. A. Jr., & Underwood, A. L. (1986) *Quantitative Analysis*, pp 118−120, Prentice-Hall, Inc., Englewood Cliffs, NJ.

Draper, D. E., Xing, R., & Laing, L. G. (1995) *J. Mol. Biol. 249*, 231−238.
Fierke, C. A., & Hammes, G. G. (1995) *Methods Enzymol. 249*, 3−37.
Frank, D. N., Harris, M. E., & Pace, N. R. (1994) *Biochemistry 33*, 10800−10808.
Gardiner, K. J., Marsh, T. L., & Pace, N. R. (1985) *J. Biol. Chem. 260*, 5415−5419.
Green, C. J., & Vold, B. S. (1988) *J. Biol. Chem. 263*, 652−657.
Guerrier-Takada, C., & Altman, S. (1984) *Science 223*, 285−286.
Guerrier-Takada, C., Gardiner, K., Marsh, T., Pace, N., & Altman, S. (1983) *Cell 35*, 849−857.
Guerrier-Takada, C., Haydock, K., Allen, L., & Altman, S. (1986) *Biochemistry 25*, 1509−1515.
Haas, E. S., Morse, D. P., Brown, J. W., Schmidt, F. J., & Pace, N. R. (1991) *Science 254*, 853−856.
Haas, E. S., Brown, J. W., Pitulle, C., & Pace, N. R. (1994) *Proc. Natl. Acad. Sci. U.S.A. 91*, 2527−2531.
Hardt, W. D., Schlegl, J., Erdmann, V. A., & Hartmann, R. K. (1993) *Nucleic Acids Res. 21*, 3521−3527.
Hardt, W. D., Warnecke, J. M., Erdmann, V. A., & Hartmenn, R. K. (1995) *EMBO J. 14*, 2935−2944.
Harris, M. E., & Pace, N. R. (1995) *RNA 1*, 210−218.
Harris, M. E., Nolan, J. M., Malhotra, A., Brown, J. W., Harvey, S. C., & Pace, N. R. (1994) *EMBO J. 13*, 3953−3963.
Haydock, K., & Allen, L. C. (1985) in *Progress in Clinical and Biological Research 172A*, pp 87−98, A. R. Liss, Inc., New York.
Holbrook, S. R., Sussman, J. L., Warrant, R. W., Church, G. M., & Kim, S. H. (1977) *Nucleic Acids Res. 4*, 2811−2820.
Johnson, K. A. (1986) *Methods Enzymol. 134*, 677−705.
Johnson, K. A. (1992) in *The Enzymes*, Vol. XX, pp 2−61, Academic Press, Orlando, FL.
Kleineidam, R. G., Pitulle, C., Sproat, B., & Krupp, G. (1993) *Nucleic Acids Res. 21*, 1097−1101.
LaGrandeur, T. E., Hüttenhofer, A., Noller, H. F., & Pace, N. R. (1994) *EMBO J. 13*, 3945-3952.
Lohman, T. M., deHaseth, P. L., & Record, M. T., Jr. (1980) *Biochemistry 19*, 3522−3530.
Lumelsky, N., & Altman, S. (1988) *J. Mol. Biol. 202*, 443−454.
Manning, G. S. (1978) *Q. Rev. Biophys. 11*, 179−286.
Manning, G. S. (1979) *Acc. Chem. Res. 12*, 443−449.
Milligan, J. F., & Uhlenbeck, O. C. (1989) *Methods Enzymol. 180*, 51−62.
Narlikar, G. J., Gopalakrishnan, V., McLConnell, T. S., Usman, N., & Herschlag, D. (1995) *Proc. Natl. Acad. Sci. U.S.A. 92*, 3668−3672.
Pace, N. R., & Smith, D. (1990) *J. Biol. Chem. 265*, 3587−3590.
Pace, N. R., & Brown, J. W. (1995) *J. Bacteriol. 177*, 1919−1928.
Pan, T. (1995) *Biochemistry 34*, 902−909.
Penefsky, H. S. (1979) *Methods Enzymol. 56*, 527−530.
Perreault, J. P., & Altman, S. (1993) *J. Mol. Biol. 230*, 750−756.
Piccirilli, J. A., Vyle, J. S., Caruthers, M. H., & Cech, T. R. (1993) *Nature 361*, 85−88.
Pyle, A. M. (1993) *Science 261*, 709−714.
Pyle, A. M., McSwiggen, J. A., & Cech, T. R. (1990) *Proc. Natl. Acad. Sci. U.S.A. 87*, 8187−8191.
Quigley, G. J., Teeter, M. M., & Rich, A. (1978) *Proc. Natl. Acad. Sci. U.S.A. 75*, 64−68.
Record, M. T., Jr., Lohman, T. M., & deHaseth, P. (1976) *J. Mol. Biol. 107*, 145−158.
Reich, C. I., Olsen, G. J., Pace, B., & Pace, N. R. (1988) *Science 239*, 178−181.
Robinson, D. R., & Grant, M. E. (1966) *J. Biol. Chem. 241*, 4030−4042.
Roselli, D. M., & Marsh, T. L. (1990) *Mol. Microbiol. 4*, 1393−1400.
Saenger, W. (1984) in *Principles of Nucleic Acid Structure*, pp 343−346, Springer-Verlag, New York.
Sambrook, J., Fritsch, E. F., & Maniatis, T. (1989) in *Molecular Cloning: A Laboratory Manual*, 2nd ed., pp 6.36−6.48, E.37−E.38, Cold Spring Harbor Laboratory Press, Plainview, New York.
Schedl, P., & Primakoff, P. (1973) *Proc. Natl. Acad. Sci. U.S.A. 70*, 2091−2095.
Schreier, A. A., & Schimmel, P. R. (1974) *J. Mol. Biol. 86*, 601−620.
Smith, D. (1995) in *The Biological Chemistry of Magnesium* (Cowan, J. A., Ed.) pp 53−83, VCH, New York.
Smith, D., & Pace, N. R. (1993) *Biochemistry 32*, 5273−5281.
Smith, D., Burgin, A. B., Haas, E. S., & Pace, N. R. (1992) *J. Biol. Chem. 267*, 2429−2436.
Steitz, T. A., & Steitz, J. A. (1993) *Proc. Natl. Acad. Sci. U.S.A. 90*, 6498−6502.
Sugimoto, N., Kierzek, R., & Turner, D. H. (1988) *Biochemistry 27*, 6384−6392.
Tallsjö, A., & Kirsebom, L. A. (1993) *Nucleic Acids Res. 21*, 51−57.
Wang, J., & Cech, T. R. (1994) *J. Am. Chem. Soc. 116*, 4178−4182.
Wang, Y.-X., Lu, M., & Draper, D. E. (1993) *Biochemistry 32*, 12279−12282.
Watanabe, S., Frantz, W., & Trottier, D. (1963) *Anal. Biochem. 5*, 345−359.
Westhof, E., & Altman, S. (1994) *Proc. Natl. Acad. Sci. U.S.A. 91*, 5133−5137.
Xing, Y., & Draper, D. E. (1995) *J. Mol. Biol. 249*, 319−331.
Zarrinkar, P. P., & Williamson, J. R. (1994) *Science 265*, 918−924.

BI960870M